Biosensors and Bioelectronics 39 (2013) 226–230

Contents lists available at SciVerse ScienceDirect

Biosensors and Bioelectronics

journal homepage: www.elsevier.com/locate/bios

Bimetallic AuPt nanochains: Synthesis and their application in electrochemical immunosensor for the detection of carcinoembryonic antigen

Xia Cao [a], Ning Wang [b,*], Shu Jia [b], Lin Guo [b], Ke Li [c]

[a] School of Biochemical and Pharmaceutical Sciences, Capital Medical University, Beijing 100069, China
[b] School of Chemistry and Environment, Beijing University of Aeronautics and Astronautics, Beijing 100083, China
[c] Department of Gastroenterology, Third Hospital of Peking University, Beijing 100083, China

ARTICLE INFO

Article history:
Received 5 May 2012
Received in revised form
20 July 2012
Accepted 23 July 2012
Available online 31 July 2012

Keywords:
AuPt alloy
Nanochain
Immunoassay
Sandwich-type
CEA

ABSTRACT

The recent development in the nanotechnology has paved the way for a large number of alloyed nanomaterials and devices of desirable properties which have useful functions for electrochemical sensor and biosensor applications. In this paper, bimetallic AuPt nanochains were synthesized through a mild chemical method, with which anti-horseradish peroxidase-conjugated anti-carcinoembryonic antigen (HRP-anti-CEA-NCAuPt) was developed for electrochemical detection of carcinoembryonic antigen (CEA) in a sandwich-type immunoassay format. The alloyed nanocrystals exhibit not only sound signal amplification effect of Au nanoparticles, but also further new combination of interfacial, electrical and structural properties arising from the disparate AuPt components. As a result, the electrochemical signal was significantly amplified by using the HRP-anti-CEA-NCAuPt as tracer and hydrogen peroxide as enzyme substrate. The linear range of the developed immunosensor is 0.01–200 ng/mL and the detection limit is 0.11 pg/mL of CEA, which makes the biometallic nanochains promising candidates for the next-generation sandwich-type electrochemical immunoassays.

1. Introduction

As a promising approach for selective and sensitive analysis with simple instrumentation, electrochemical immunoassay has gained much attention in the quantitative detection of tumor markers and screening of cancers (Bosker and Huestis, 2009; Wu et al., 2007; Martinez et al., 2010; Chikkaveeraiah et al., 2009).

During the past decade, the reduction in size of functional architectures has been a dominating trend in many fields of science and technology. Structural size reduction down to the nanometer scale leads not only to a miniaturization of functional units, but also to the development of new sensing materials with unique physical and chemical properties for the application in novel electrochemical systems (Martinez et al., 2010; Chikkaveeraiah et al., 2009; Gas et al., 2010; Wu et al., 2009; Vericat et al., 2010; Tang et al., 2005; Mozaffari et al., 2010; Shim et al., 2008; Kim et al., 2008).

For example, while gold nanoparticles (Au NPs) have been widely used for promoting the electrochemical transportation or as carriers for loading numerous signal tags with acceptable function of signal amplification, bimetallic nanoparticles are also attracting increasing attention because of their feature interesting catalytic behaviors (Chen et al., 2012; Gholivand and Azadbakht, 2011; Gholivand et al., 2011; Tong et al., 2010; Xiao et al., 2009). Compared with single metal NPs, bimetal NPs present distinct characteristics, in which one metal takes on a long-term stability and biocompatibility, and the other shows the specific optical or electrical activity to be monitored. Most reports on bimetallic NPs are related to the combination of Au with another metal, such as Ag, Pd, Ru, and Pt (Chen et al., 2012; Gholivand and Azadbakht (2011); Gholivand et al., 2011; Tong et al., 2010; Xiao et al., 2009; Mayorga et al., 2012; Tsai et al., 2010; Upadhyay et al., 2009). In these works, bi-metallic electrodes typically provide a rapid response, good stability, electrocatalytic capability and reproducibility for the selected target detection. Furthermore, efforts have been devoted to the assemblies of spherical or pseudo-spherical nanostructures, where the sensing properties of nanoparticles are controlled not only by the size, composition, and geometry, but also by the spatial arrangement of the nanoparticle building blocks (Mayorga et al., 2012). Typically, wired nanoparticles could be an ideal substrate for growing and anchoring of functional molecules for high-performance electrocatalytic or electrochemical devices due to the enhanced electron transport rate, high electrolyte contact area, and structural stability.

Herein, bimetallic AuPt nanochains (NCAuPt) were synthesized through a mild chemical method. A nanolabel based on NCAuPt conjugated HRP-anti-CEA (HRP-anti-CEA-NCAuPt) was designed for an electrochemical immunosensor to detect CEA in clinical diagnosis. The potential of bimetallic nanochains for

* Corresponding author. Fax: +86 10 82338162.
E-mail address: wangning@buaa.edu.cn (N. Wang).

0956-5663/$ - see front matter © 2012 Elsevier B.V. All rights reserved.
http://dx.doi.org/10.1016/j.bios.2012.07.046

sandwich-type electrochemical immunoassays was expected due to their highly amplified properties.

2. Experimental

2.1. Material

Mouse monoclonal anti-CEA (clone no.10), HRP-anti-CEA and CEA were purchased from Sigma (USA). $HAuCl_4 \cdot 4H_2O$, $HPtCl_6$, and bovine serum albumin (BSA, 96–99%) were purchased from Sigma–Aldrich and used as received. All other reagents, unless otherwise stated, were of analytical grade and were purchase from Sinopharm Chemical Reagent Beijing Co. Ltd used without further purification. Double distilled water was used throughout the experiment. Clinical serum samples were provided by the Third Hospital of Peking University.

2.2. Synthesis of ultrathin NCAuPt

For the growth of NCAuPt, 8.5 mg of sodium boronhydride (dissolved in 20 mL of pure water) was dropped in to 8.5 mg of $NiCl_2 \cdot 6H_2O$, 50 mg of polyvinylpyrrolidone (K30, dissolved in 40 mL of water). Immediately after the addition of sodium boronhydride, a mixture of 0.0024 g of $H_2PtCl_6 \cdot 4H_2O$, and 0.0010 mg of $HAuCl_4 \cdot 4H_2O$ (dissolved in 20 mL of 0.05 M HCl) were quickly added. The mixture was sonicated for 30 min, and then was kept under constant stirring at 60 °C for 2 h. All the steps were carried out under the protection of Nitrogen. The resulting solid AuPt nanomaterials were collected by centrifugation and washed with water for six cycles, then dried in air for characterization. The Au and Pt NCs were also synthesized by the standard procedure for comparison, either in the absence of H_2PtCl_6 (for Au nanochains) or without the addition of H_2AuCl_6 (for Pt chains), respectively.

2.3. Preparation of HRP-anti-CEA-NCAuPt nanolabels and electrochemical immunosensor

The synthetic procedure of HRP-anti-CEA-NCAuPt is illustrated in Fig. 1A, based on the conjugation of NCAuPt to HRP-anti-CEA via the reaction with amine groups of proteins. Typically, 2.0 mL NCAuPt (25 mg/mL) were initially added in 10 mL PBS and the pH adjusted to 9.5 using 10% (w/v) K_2CO_3, and then 500 μL HRP-anti-CEA (500 ng/mL) was injected into the mixture and incubated for 12 h at 4 °C with slight stirring. The mixture was centrifuged at 8000 rpm for 10 min. Then the precipitate was added into BSA solution to block possible remaining active sites of the NCAuPt and avoid the non-specific adsorption. The resulting mixture was centrifuged at 4000 rpm for 15 min. The prepared HRP-anti-CEA-NCAuPt was then stored in phosphate buffered saline (PBS, pH 7.4) at 4 °C. For comparison, HRP-anti-CEA-NCAu and HRP-anti-CEA-NCPt and HRP-anti-CEA were also prepared. Preparation process of the immunosensor is similar to that reported previously (Zhong et al., 2010) as shown in Fig. 1B.

2.4. Measurement protocol

The electrochemical detection of CEA was based on a competitive immunoassay format. A schematic diagram of the procedure is shown in Fig. 1C. The immunosensor was initially incubated with various concentrations of CEA standards/specimens for 30 min at RT, and then the resulting immunosensor was submerged into HRP-anti-CEA-NCAuPt (25 mg/mL) or HRP-anti-CEA-NCAu, HRP-anti-CEA-NCPt, HRP-anti-CEA nanolable solution for another 30 min at room temperature with slight stirring (150 rpm). After rinsing thoroughly with PBS (pH 7.0) to remove the unbound secondary antibodies, amperometric responses of the immunosensor were recorded using cyclic voltammetry at 50 mV/s in PBS (pH 6.9) containing 0.8 mM $\cdot H_2O_2$ due to the catalytic reduction of the bound HRP toward H_2O_2.

2.5. Characterizations

The as-synthesized NCAuPt and HRP-anti-CEA-NCAuPt was characterized by transmission electron microscopy (TEM) (JEM 2100 F). All the electrochemical tests were carried out at room temperatures under nitrogen atmosphere on a CHI 660C electrochemical station, using a single compartment, three-electrode cell. Electrode potentials were measured with respect to an aqueous saturated calomel electrode (SCE). A Pt wire was used as the counter electrode.

3. Results and discussion

3.1. Characteristics of NCAuPt and HRP-anti-CEA-NCAuPt nanolabel

The morphology of the as-synthesized AuPt nanomaterials was examined by TEM. As can be seen from Fig. 2A, the AuPt product consists of chained nanoparticles with sizes of about 3–5 nm.

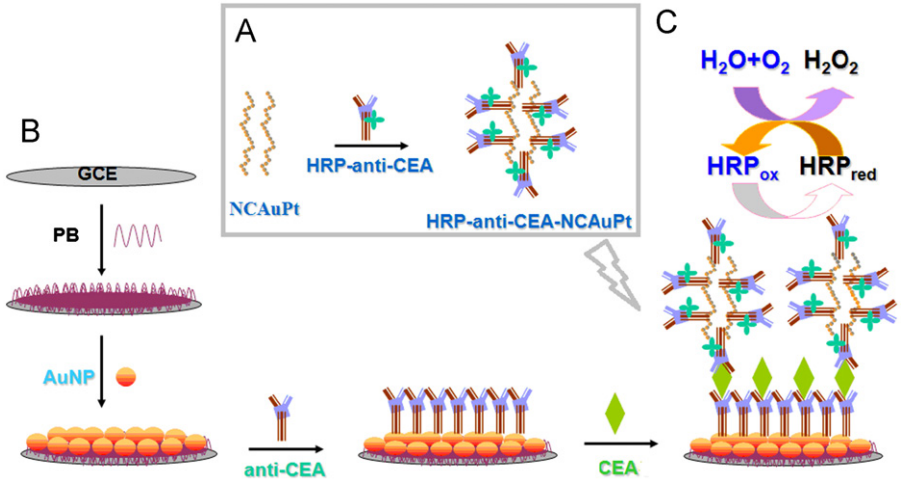

Fig. 1. Schematic illustration of the preparation of the HRP-anti-CEA-NCAuPt nanolabel (A), the sandwich-type electrochemical immunosensor (B), and measurement protocol (C).

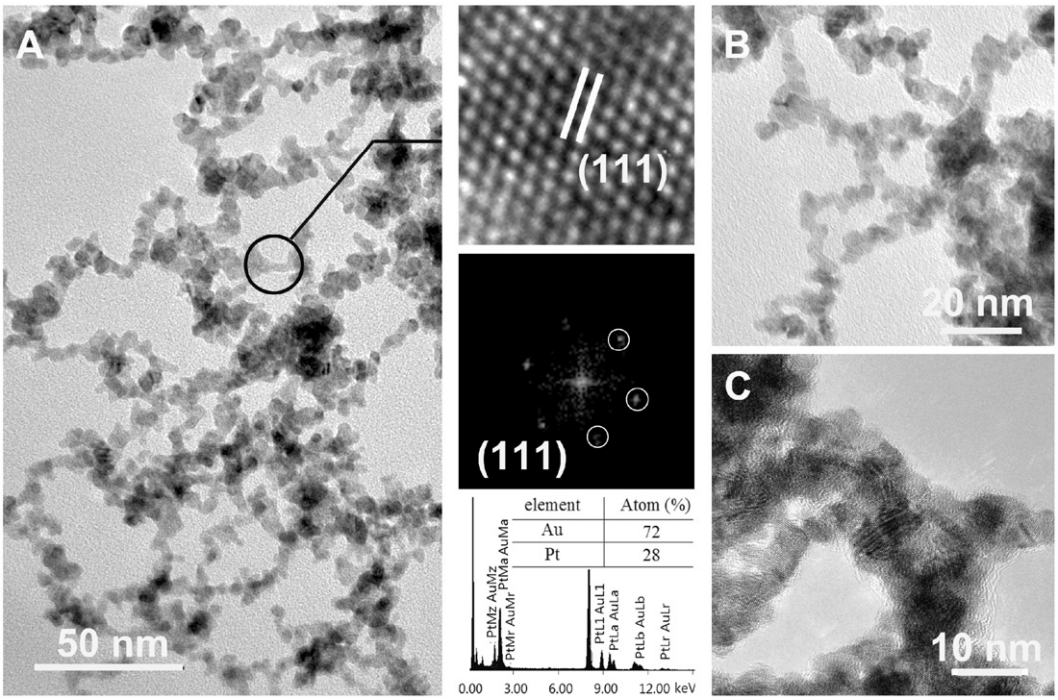

Fig. 2. Typical TEM image the NCAuPt: TEM images of NCAuPt (A), (B) and HRP-anti-CEA-NCAuPt (C). Insets of Fig. 2A are HRTEM (Up inset), FFT pattern (middle inset) and EDS spectrum (down inset) of the NCAuPt.

These particles are grown in close contact with each other, forming branched nanochains with a length of hundreds of nanometers. Detailed information was given by a high resolution TEM (Up inset of Fig. 2A). The nanochains were made up of single-domain crystals. Visible lattice fringes of 0.23 nm and 0.20 nm can be calculated (0.229 nm, 0.195 nm), matching well with the expected *d*-spacing of (1 1 1) and (2 0 0) planes of the Au_5Pt_2 alloy. The slight spacing shifts indicate that the crystal structure was a substitution solid solution of Au_5Pt_2 with a lattice constant of 0.397 nm, as was further proved by the energy-dispersive X-ray spectrum (EDS, down inset Fig. 2A) and fast Fourier transformation pattern (FFT, middle inset Fig. 2A). The TEM images show that the nanochains were uniformly coated with an amorphous thin layer after conjugation of NCAuPt to HRP-anti-CEA (Fig. 2B and C), and the coverage density of HRP-anti-CEA can be easily tuned by changing the HRP-anti-CEA concentration or the incubation time.

3.2. Electrochemical behavior of immunosensors

HRP can be used for amplification of electrochemical immunoassay signal through enzymatic reduction of H_2O_2 with ferrocene or its derivates as electron transfer mediator. To investigate the effect of the synthesized NCAuPt on the sensitivity of the electrochemical immunosensors, four types of conjugated antibodies (HRP-anti-CEA-NCAu, HRP-anti-CEA-NCPt, HRP-anti-CEA-NCAuPt and HRP-anti-CEA) were prepared. Different concentrations of CEA were assayed using various labeled probes and the same batch immunosensors. The judgment is based on the amperometric change of the immunosensor before and after the antigen–antibody interaction. Cyclic voltammograms of the electrochemical immunoassay using various detection antibodies such as HRP-anti-CEA-NCAu, HRP-anti-CEANCPt, HRP-anti-CEA-NCAuPt and HRP-anti-CEA in the absence (solid) and presence (hollow) of 0.8 mM · H_2O_2 after reaction with 50 ng/mL CEA in PBS (pH 6.9) were shown in Fig. 3A–D, sequentially. Upon the addition of H_2O_2 into the substrate solution, obvious catalytic characteristics appeared with a distinct increase of the reduction current and a decrease of the oxidation current. The catalytic current is mainly resulted from the labeled HRP toward the reduction of H_2O_2 with the help of the electrodeposited Prussian blue (PB) as electron mediator. When HRP-anti-CEA bound onto the NCAu (Fig. 3A), NCPt (Fig. 3B), and NCAuPt (Fig. 3C) surfaces reacted with the corresponding antigen (analyte), the carried HRP molecules exhibited higher catalytic efficiency relative to the H_2O_2 system than that of directly using HRP-anti-CEA labeled secondary antibody (Fig. 3D). In addition, compared with HRP-anti-CEA-NCAu and HRP-anti-CEA-NCPt, the use of HRP-anti-CEA-NCAuPt showed almost two-fold higher electrocatalytic response (Fig. 3C), indicating the acceleration of electron transfer by NCAuPt. This performance enhancement may be ascribed to the structural characteristics of the NCAuPt. Generally, the strong interconnection of the orderly assembled particles can both eliminate randomness of the grain network and increase contact points for good electrical connection. In comparison to their single-composition counterparts, such alloyed NCAuPt catalysts present not only enhanced scattering of free electrons and mass transfer, but also synergistic characteristics. In this case, Au takes on the sound biocompatibility, and the alloyed AuPt NCs promotes the specific surface area, electron transfer as well as the long-term structural stability due to direct electronic interaction and geometric strain. As a result, the high surface-to-volume ratio of NCAuPt can greatly enhance the amount of immobilized HRP-anti-CEA, while charge carrier recombination will be reduced in HRP-anti-CEA-NCAuPt based nanolabels.

3.3. Optimization of the immunoassay procedure

The effect factors of the immunoassay procedure such as the optimal pH value of the solution, the time and temperature of incubation for the immune-reaction were also examined in this work. Fig. 4 (curve a) shows the effect of pH of the detection solution on the current responses of the immunoassay in the presence of 0.8 mmol/L H_2O_2 toward 50 ng/mL CEA. The current

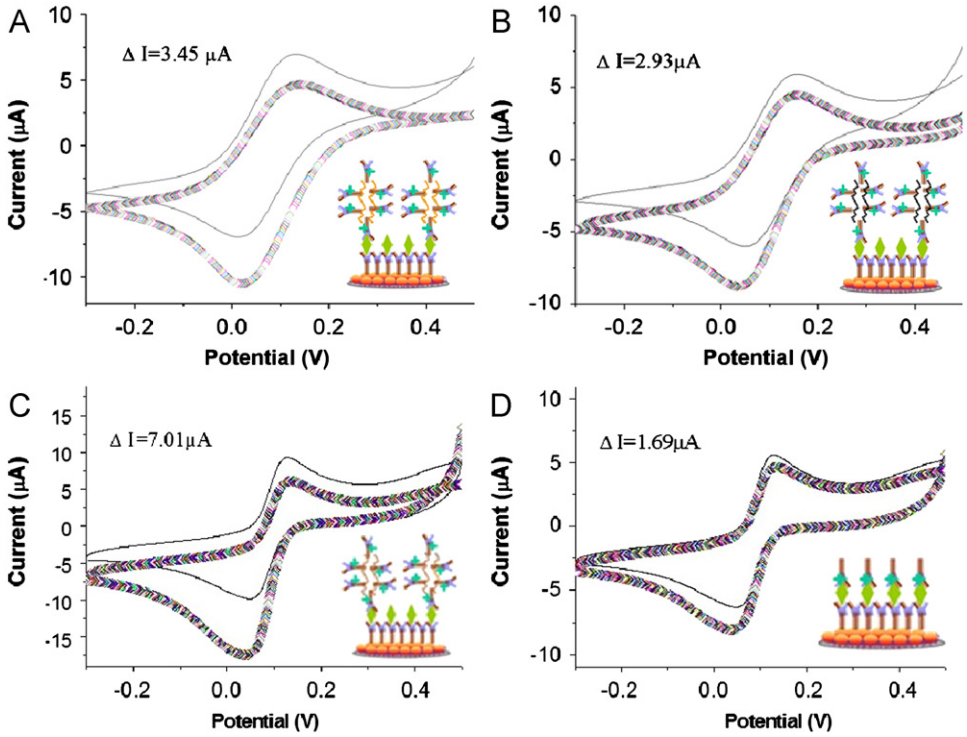

Fig. 3. Cyclic voltammograms of the electrochemical immunoassay using various detection antibodies: (A) HRP-anti-CEA-NCAu, (B) HRP-anti-CEA-NCPt, (C) HRP-anti-CEA-NCAuPt and (D) HRP-anti-CEA in the absence (solid) and presence (hollow) of 0.8 mM H_2O_2 after reaction with 50 ng/mL CEA in PBS (pH 6.9).

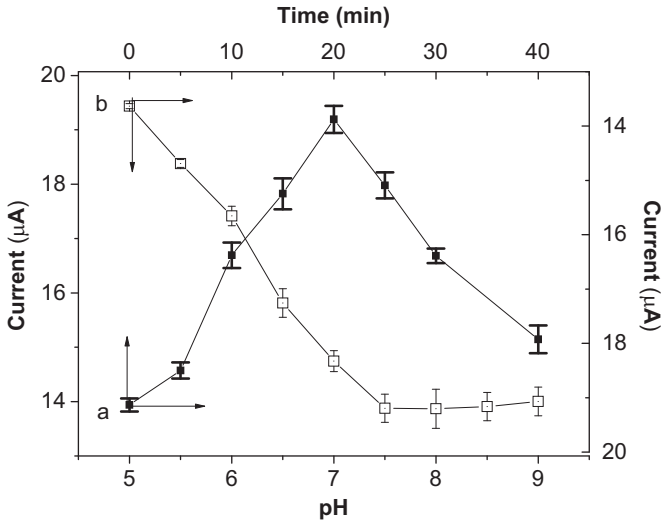

Fig. 4. Effects of pH of detection solution (curve a) and incubation time (curve b) on peak current responses to 50 ng/mL CEA at the immunosensor array.

change was increased with the increment of pH value from pH 4.9 to 6.9 and then decreased. The optimal amperometric response was achieved at pH 6.9. The reason is that highly acidic or alkaline surroundings would damage the immobilized protein, especially in alkalinity. Thus, pH 6.9 was selected for the electrochemical immunoassay. The time and temperature of the antigen–antibody reaction also greatly affected the analytical performance of the proposed immunoassay. The amperometric response increased with an increment of incubation temperature from 10 to 50 °C and reached a plateau at 35 °C (not shown here). To simplify the analytical process, all the experiments were carried out at room temperature. The amperometric response of the immunoassay increased with the incubation time and leveled off after 25 min (Fig. 4, curve b). Longer incubation time did not improve the response. Therefore, 25 min was selected as the incubation time for the determination of CEA antigen in this study.

3.4. Analytical performance

To assess the sensitivity and the linear range of the proposed immunoassay, routine samples of different CEA concentrations were assayed with linear-sweep stripping voltammetry using the HRP-anti-CEA-NCAuPt as tracer and H_2O_2 as enzyme substrate under optimal conditions. As shown in Fig. 5, the current responses increased with the increment of CEA concentration in the sample solution after the antigen antibody interaction in PBS (pH 6.9). The current variations showed a linear relationship with the concentration of CEA over the range of 0.01 – 200 ng/mL with a detection limit of 1.1 pg/mL at a signal-to-noise ratio of 3, which is lower than 6.7 pg/mL (Tang and Ren, 2008) 10 pg/mL (Zhong et al., 2010) 32 pg/mL (Ho et al., 2009), and 0.01 ng/mL (Wilson and Nie, 2006; Chen et al., 2010) reported in previous studies. It can be deduced that the wired nanoalloys exhibit not only a combination of electrical and interfacial properties from the disparate metal components, but also further novel synergistic catalysis, adsorbing and sensing performance that arise from the interactions between the Au and Pt components. As a result, the use of HRP-anti-CEA-NCAuPt as detection antibodies could significantly amplify the signal of the immunosensors. Ultrahigh sensitivity of the immunoassay could be obtained through the enzymatic signal amplification of high-content HRP and the presence of NCAuPt on immunosensor surface.

3.5. Reproducibility, Specificity and Stability

The reproducibility of the response of the immunosensors was examined by analysis of the same concentration of CEA (50 ng/mL) using five parallelly prepared electrodes. The five immunosensors, made independently, showed the current responses of

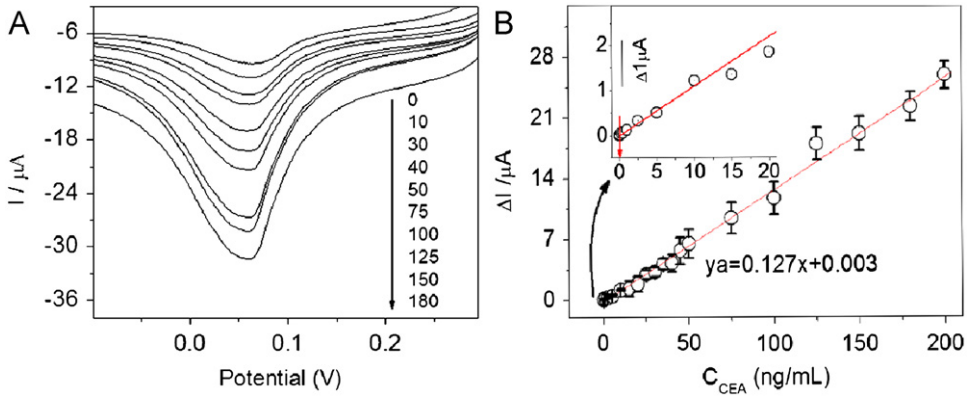

Fig. 5. LSV curves (A) and calibration curves (B) for the electrochemical immunosensor toward CEA at different concentrations using HRP-anti-CEA-NCAuPt detection antibodies in PBS (pH 6.9) containing 0.8 mM H_2O_2.

17.36, 17.61, 17.85, 17.24, 18.17 μA. It was observed that the immunosensor had acceptable reproducibility with a relative standard deviation of less than 5.0%.

Specificity is one of the potential advantages of using biological molecules as recognition elements in immunosensor. Other possible interferents such as α-fetoprotein (AFP), human chorionic gonadotrophin (HCG), and BSA, were used to evaluate the selectivity of immunosensors. The immunosensors were separately exposed to 10 ng/mL CEA solutions with interference (40 ng/mL) and without interference. It was found that the relative standard deviations (RSD) were 0.88%, 0.69%, and 0.96%, respectively. The result indicates that the selectivity of the as-prepared immunosensor was acceptable within experimental error.

The stability of HRP-anti-CEA-NCAuPt was also examined. When the HRP-anti-CEA-NCAuPt was not in use, it was stored in PBS (pH 6.9) at 4 °C. It retained 90.1% of its initial response after 1 month of storage. The slow decrease of response might due to the destructibility of the HRP-anti-CEA-NCAuPt.

3.6. Accuracy and clinical application

The accuracy of CEA detection was examined by comparing the analytical results of four serum samples with this method and enzyme-linked immunosorbent assay method (ELISA), as shown in Table 1 in the supporting material. The two methods were in acceptable agreement. The errors indicated that the sensor performed well in the detection of CEA in serum and most of the results were accurate and credible.

4. Conclusions

In brief, bimetallic NCAuPt were synthesized through a mild chemical method and an electrochemical immunoassay for CEA measurement was designed. The alloyed nanocrystals exhibit not only a combination of electrical and interfacial properties from the disparate metal components, but also further novel synergistic adsorbing and sensing properties that arise from the interactions between the AuPt components. As a result, analytical sensitivity of the assay was greatly increased by the NCAuPt encapsulated with the secondary HRP-anti-CEA antibody label in a sandwich enzyme immunoassay format. Although the present assay system is focused on the determination of the target antigen molecules, it can be easily extended to the detection of other antigens or bio-compounds. It possesses acceptable detection and storage stability for fabrication in batch.

Acknowledgements

This work was supported by the National Natural Science Foundation of China (No. 21173017, 50902007, & 21275102), the Natural Science Foundation of Jiangsu Province (No. BK2010341), and the 973 Program (2010CB934701).

Appendix A. Supporting information

Supplementary data associated with this article can be found in the online version at http://dx.doi.org/10.1016/j.bios.2012.07.046.

References

Bosker, W.M., Huestis, M.A., 2009. Clinical Chemistry 55, 1910–1931.
Chen, H.F., Tang, J.A., Su, B., Chen, G., Huang, J.X., Tang, D.P., 2010. Analytica Chimica Acta 678, 169–175.
Chen, K.J., Pillai, K.C., Rick, J., Pan, C.J., Wang, S.H., Liu, C.C., 2012. Biosensors and Bioelectronics 33, 120–127.
Chikkaveeraiah, B., Bhirde, A., Malhotra, R., Patel, V., Gutkind, J.S., Rusling, J.F., 2009. Analytical Chemistry 81, 9129–9134.
Gas, F., Baus, B., Pinto, L., Compere, C., Tanchou, V., Quéméneur, E., 2010. Biosensors and Bioelectronics 25, 1235–1239.
Gholivand, M.B., Azadbakht, A., Pashabadi, A., 2011. Electroanalysis 23, 2771–2779.
Gholivand, M.B., Azadbakht, A., 2011. Electrochimica Acta 56, 10044–10054.
Ho, J.A., Lin, Y.C., Wang, L.S., Hwang, K., Chou, P.T., 2009. Analytical Chemistry 81, 1340–1346.
Kim, E.Y., Stanton, J., Korber, B.T., Krebs, K., Bogdan, D., Kunstman, K., 2008. Nanomedicine 3, 293–303.
Martinez, N.A., Schneider, R.J., Messina, G.A., Raba, J., 2010. Biosensors and Bioelectronics 25, 1376–1381.
Mozaffari, S.A., Chang, T., Park, S.M., 2010. Biosensors and Bioelectronics 26, 74–79.
Mayorga, C., Guix, M., Madrid, R.E., Merkoci, A., 2012. Chemical Communications 48, 1686–1688.
Shim, S.Y., Lim, D.K., Nam, J.M., 2008. Nanomedicine 3, 215–232.
Tang, D.P., Yuan, R., Chai, Y.Q., Liu, Y., Dai, J.Y., Zhong, X., 2005. Analytical and Bioanalytical Chemistry 381, 674–680.
Tong, S.F., Xu, Y.H., Zhang, Z.X., Song, W.B., 2010. Journal of Physical Chemistry C 114, 20925–20931.
Tsai, T.H., Thiagarajan, S., Chen, S.M., 2010. Journal of Applied Electrochemistry 40, 2071–2076.
Tang, D.P., Ren, J.J., 2008. Analytical Chemistry 80, 8064–8070.
Upadhyay, S., Rao, G.R., Sharma, M.K., Bhattacharya, B.K., Rao, V.K., Vijayaraghavan, R., 2009. Biosensors and Bioelectronics 25, 832–838.
Vericat, C., Vela, M.E., Benitez, G., Carro, P., Salvarezza, R.C., 2010. Chemical Society Reviews 39, 1805–1834.
Wilson, M.S., Nie, W.Y., 2006. Analytical Chemistry 78, 6476–6483.
Wu, J., Yan, F., Tang, J.H., Zhai, C., Ju, H.X., 2007. Clinical Chemistry 53, 1495–1502.
Wu, S., Zhong, Z.Y., Wang, D., Li, M.X., Qing, Y., Dai, N., 2009. Microchimica Acta 166, 269–275.
Xiao, F., Zhao, F.Q., Mei, D.P., Mo, Z.R., Zeng, B.Z., 2009. Biosensors and Bioelectronics 24, 3481–3486.
Zhong, Z., Wu, W., Wang, D., Wang, D., Shan, J., Qing, Y., 2010. Biosensors and Bioelectronics 25, 2379–2383.